N6-methyladenosine-related lncRNAs as a biomarker for predicting the prognosis and immune microenvironment of clear cell renal cell carcinoma

Yuqin Qiu
Beijing University of Chinese Medicine
Xiaogang Wang
Beijing Haidian Section of Peking University Third Hospital: Beijing Haidian Hospital
Zhenjia Fan
Beijing University of Chinese Medicine
Shanhui Zhang
Beijing University of Chinese Medicine
Jinchang Huang (zryhhuang@163.com)
Beijing University of Chinese Medicine
Xin Jiang
Beijing University of Chinese Medicine Third Affiliated Hospital

Research

Keywords: N6-Methyladenosine, long non-coding RNA, clear cell renal cell carcinoma, prognosis, immune checkpoint, immune cell infiltration

Posted Date: March 22nd, 2021

DOI: https://doi.org/10.21203/rs.3.rs-339064/v1

Abstract

Background: Patients with advanced clear cell renal cell carcinoma (ccRCC) have a poor prognosis and lack effective prognostic biomarkers. This study uses bioinformatics analysis to identify N6-methyladenosine-related lncRNAs (m6A-related lncRNAs) as new prognostic biomarkers for ccRCC.

Methods: Gene expression data and related clinical information of ccRCC patients were extracted from the Cancer Genome Atlas Database. m6A-related lncRNAs were obtained by co-expression analysis. Univariate Cox regression analysis was performed on these lncRNAs to find the prognostic-related m6A-related lncRNAs, and consensus clustering analysis was performed. The prognostic signature was screened by LASSO regression and a prognostic model was constructed. The predictive performance of the prognostic model was evaluated and validated by survival analysis and ROC curve analysis, etc. In addition, we also systematically analyzed the expression of immune checkpoints and immune cell infiltration in ccRCC patients.

Results: First, 27 m6A-related lncRNAs associated with prognosis were identified, which were significantly differentially expressed between tumor and normal tissues. Consensus clustering analysis indicated that cluster 2 was associated with poor prognosis, low stromal score, high expression of *PD-1, PD-L1, CTLA-4, LAG-3, TIM-3, TIGIT*, and immunosuppressive cell infiltration. The signaling pathways related to tumor progression, drug resistance, and angiogenesis and biological processes related to protein methylation and phosphatidic acid metabolism are significantly enriched in cluster 2. Subsequently, LASSO regression analysis was used to construct a prognostic risk model based on 7 m6A-related lncRNAs signature, which can be used as an independent prognostic indicator. After a series of analyses, it was shown that this model had good sensitivity and specificity, can predict the prognosis of patients with different clinical stratifications and was associated with the progression of ccRCC. The expression levels of immune checkpoints were significantly increased in high-risk patients, and there was a certain correlation between the risk score and immune cell infiltration.

Conclusions: In summary, we constructed and validated a risk model that can independently predict the prognosis of ccRCC patients and reflect the immune microenvironment based on m6A-related lncRNAs; the model is conducive to the screening of biomarkers of ccRCC prognosis and may have the potential to reflect the response of ccRCCs to immunotherapy.

Background

Renal cell carcinoma (RCC) is a common genitourinary tumor, and its incidence has increased year by year, accounting for 3%-5% of adult malignancies, and is higher in men than in women [1]. Clear cell renal cell carcinoma (ccRCC) is the most common pathological type of RCC, accounting for approximately 75% of RCCs [2]. The classical RCC triad is hematuria, flank pain, and abdominal masses. However, most RCC patients are asymptomatic at onset and are already at an advanced stage at the time of diagnosis. Although the 5-year survival rate of early RCC is 93%, the prognosis of patients with locally advanced or

metastatic RCC is generally poor, and the 5-year survival rate is only approximately 12% [3-4]. Therefore, an effective prognostic marker is of great significance for early diagnosis and treatment as well as for improving patient prognosis. ccRCC is resistant to traditional radiotherapy and chemotherapy, and the treatment methods for patients with advanced ccRCC are very limited. Targeted drugs such as sorafenib are the standard means of treatment for advanced stage patients. In recent years, some clinical studies have demonstrated that immunotherapy is effective for advanced RCC [5-6]. As people's awareness of tumor immunity continues to rise, novel immunotherapeutic drugs continue to emerge. Searching for novel biomarkers is critical for the better selection of patients who may benefit most from these treatments [7].

Long non-coding RNAs (lncRNAs) are a group of noncoding RNAs with a length greater than 200 nucleotides [8]. They can regulate gene expression through epigenetic regulation, transcriptional regulation and posttranscriptional regulation and are involved in biological processes such as the regulation of tumor cell cycle, cell proliferation, differentiation, apoptosis and migration [9-11]. An increasing number of lncRNAs have been shown to be abnormally expressed in cancers and have a significant correlation with treatment and clinical prognosis, providing the possibility for lncRNAs to become novel tumor biomarkers and therapeutic targets [12]. For example, the level of lncRNA *small nucleolar RNA host gene 14 (SNHG14)* is significantly increased in ovarian cancer tissues, and the inhibition of *SNHG14* significantly inhibits the migration and invasion of cells [13]. The upregulation of the lncRNA *gastric cancer metastasis associated long noncoding RNA (GMAN*) in gastric cancer tissues is associated with metastasis in patients [14]. The lncRNA *Urothelial cancer associated 1 (UCA1)* is significantly upregulated in RCCs and is positively correlated with tumor differentiation and tumor-node-metastasis (TNM) staging; it promotes the malignant phenotype of RCCs through the regulation of the miR-182-5p/DLL4 axis [15].

N6-methyladenosine (m6A) is methylation that occurs in the N6-position of adenosine [16]. It was first discovered in eukaryotic messenger RNA (mRNA) in 1970 and is considered to be the most common and abundant RNA modification [17]. m6A modification is a reversible and dynamic process. It is regulated by 3 types of m6A regulators. m6A is catalyzed by methyltransferases (called “writers”, such as *METTL3, METTL14,* and *RBM15),* is removed by demethylases (called “erasers”, such as *FTO* and *ALKBH5*), and is recognized by binding proteins (called “readers”, such as *YTHDC1-2 and YTHDF1-3*), thereby regulating RNA metabolism [16-17]. m6A modification has been confirmed to be involved in the regulation of the occurrence and progression of a variety of cancers, including ccRCC and breast cancer [18-19]. Studies have shown that lncRNAs are also widely modified by m6A [20] and that the interaction between the two is involved in tumor progression, metastasis, drug resistance and immune responses [21]. Studies have reported that m6A-related lncRNAs can be used as potential biomarkers to predict the prognosis of patients with glioma [22]. However, the biological role of the interaction between lncRNA expression and m6A-related genes in ccRCC has not been explored. Therefore, we used bioinformatics to screen for m6A-related lncRNAs that are closely related to ccRCC prognosis and constructed a prognostic model. We hope that our results will help to better assess the prognosis of ccRCC patients and guide clinical

treatment. Our results also provide a basis for further exploration of the potential mechanism of m6A modification of lncRNAs in ccRCC.

Materials And Methods

Data acquisition and collation

Transcriptomic sequencing (RNA-seq) data, fragments per kilobase of transcript per million mapped reads (FPKM), and related clinical information of ccRCC patients were downloaded from The Cancer Genome Atlas (TCGA) database (https://portal.gdc.cancer. gov/). The Genome Reference Consortium Human Build 38 (GRCh38) was downloaded from GENCODE (https://www.gencodegenes.org/human), and the expression data of lncRNAs in the transcriptome were extracted based on the gene biotype. These data were obtained from public databases, and therefore, ethics approval was not required.

Extraction of m6A-related lncRNAs associated with prognosis

By reviewing published studies, we found 23 m6A-related genes, namely, methyltransferases *METTL3, METTL14, METTL16, WTAP, VIRMA, ZC3H13, RBM15, and RBM15B*; demethylases *ALKBH5* and *FTO;* and recognition proteins *YTHDC1. YTHDC2, YTHDF1, YTHDF2, YTHDF3, HNRNPC, FMR1, LRPPRC, HNRNPA2B1, IGFBP1, IGFBP2, IGFBP3,* and *RBMX* [23-24]. The expression matrix of m6A-related genes in ccRCC samples was extracted from TCGA transcriptome data. Coexpression analysis was performed for m6A-related genes and lncRNAs by calculating the Person correlation coefficient; the filtered correlation coefficient was > 0.7, $p < 0.001$. These lncRNAs were combined with clinical survival data to identify the m6A-related lncRNAs associated with ccRCC prognosis via univariate Cox regression analysis.

Biological characteristics of m6A-related lncRNAs

To investigate the clinical significance of m6A-related lncRNAs associated with prognosis, we used the Consensus Clustering algorithm and the ConsensusClusterPlus package [25] of R, version 4.0.3, to classify ccRCC patients into different subtypes based on the expression levels of prognosis-related lncRNAs. The differences in clinical features and prognosis were analyzed. Consensus clustering is a method that provides quantitative evidence for determining the membership and number of possible clusters in a dataset and is widely used in cancer genomics. Because resampling was used, the obtained clustering results had excellent stability.

To further explore the biological processes mediated by m6A-related lncRNAs, we used GSEA software (version 4.1.0) to determine gene expression enrichment for different subtypes in the Molecular Signatures Database (MSigDB) Collection (c5.go.bp.v7.2.symbols.gmt; c2.cp.kegg. v7.2symbols.gmt) to analyze the difference between GO functional enrichment and KEGG pathway enrichment. A normalized enrichment score (NES) > 1 and nominal p-value (NOM p-val) < 0.05 were used to determine the difference between different genotypes.

Correlation analysis of m6A-related lncRNAs and immune checkpoints

To investigate the indication effect of m6A-related lncRNAs in immunotherapy for ccRCC, the differential expression of key genes associated with currently used tumor immune checkpoint inhibitors, including programmed cell death 1 *(PD-1),* programmed cell death-Ligand 1 *(PD-L1),* cytotoxic T lymphocyte-associated antigen 4 *(CTLA-4),* lymphocyte activation gene-3 *(LAG-3),* T cell immunoglobulin and mucin domain-containing protein 3 *(TIM-3)* and T cell immunoglobulin and ITIM domain (*TIGIT)*, was compared in tumor and normal samples and among different clusters using the limma package of R software [26]. The corrplot package [27] was used to visualize the coexpression relationship between the above genes and m6A-related lncRNAs associated with prognosis.

Correlation analysis of m6A-related lncRNAs and the immune microenvironment

To analyze the effect of m6A-related lncRNAs on the tumor immune microenvironment, we used the CIBERSORT algorithm [28] to evaluate the immune cell infiltration of different clusters. CIBERSORT is a tool for the deconvolution of the expression matrix of human immune cell subtypes based on the principle of linear support vector regression. Immune cell infiltration can be estimated by RNA-seq data. Leukocyte signature matrix (LM22) contains 547 genes that distinguish 22 human immune cell phenotypes, including seven T cell types, naive and memory B cells, plasma cells, NK cells, and myeloid subsets. We used the CIBERSORT algorithm to analyze the RNA-seq expression profile based on LM22 classification. We evaluated the abundance of immune cell subsets in samples and visualized the differences in immune cell infiltration between different types. In addition, we used the ESTIMATE algorithm in the R estimate package [29] to calculate the ratio of immune cells and stromal cells in the tumor microenvironment (TME) for each sample to evaluate tumor purity.

Construction and validation of the prognostic risk model

First, the Caret package [30] was used to randomly divide the samples with complete survival information in the TCGA database into 2 groups, i.e., a training set and a test set, with each set consisting of approximately 50% of cases. Subsequently, LASSO regression analysis was used to construct the prognostic model. The optimized model was obtained using the penalty parameter estimated by 10-fold cross-validation. The risk score of the prognostic model = , where *Coef* represents the regression coefficient, and β represents the m6A-related lncRNA expression value. The risk score for each patient was calculated using the formula, and then, the training set and test set were divided into a high-risk group and a low-risk group based on the median score. The R survival package was used for Kaplan-Meier analysis. The log-rank test was used to compare the overall survival rates for the high- and low-risk groups. A time-dependent receiver operating characteristic (ROC) curve was plotted. Area under the curve (AUC) > 0.60 was considered an acceptable prediction. In addition, we also used univariate and multivariate Cox regression analyses to assess whether the risk score could be an independent prognostic factor for ccRCC. To evaluate the predictive ability of the model for different populations, Kaplan-Meier analysis was performed for age, sex, grade, stage, and TNM staging. Finally, we analyzed the correlation between risk scores and clinicopathological features to assess the ability of this model to predict ccRCC progression.

Analysis of immune differences in patients with different prognostic risks

To understand the significance of this risk model in the assessment of the immune microenvironment and immunotherapeutic efficacy in ccRCC, we analyzed the differences in immune checkpoint expression between high- and low-risk patients and the correlation between risk scores and tumor-infiltrating immune cells.

Results

Identification of m6A-related lncRNAs associated with ccRCC prognosis

The RNA-seq data of 611 samples (tumor samples, 539; normal samples, 72) downloaded from TCGA were combined with GRCh38 downloaded from GENCODE to obtain 14086 lncRNAs. Person correlation analysis of the expression matrix of these lncRNAs and m6A-related genes yielded a total of 239 lncRNAs that were significantly positively correlated with *RBM15* and *METTL3* (Figure 1A, Table S1). Through univariate Cox regression analysis, 27 m6A-related lncRNAs significantly correlated with prognosis were obtained ($p < 0.001$, Figure 1B, Table S2). The expression levels of these lncRNAs were significantly different between ccRCC tumor tissue and normal tissue (Figure 1C, D). Three low-risk lncRNAs, *AC018752.1, RPL34-AS1* and *COL18A1-AS1*, had higher expression in normal tissue than in tumor tissue, and the remaining 24 high-risk lncRNAs (*AC084018.1, AC012615.6, AC114730.3, AL008718.3, LINC00342, AL136295.7, AC004148.1, AL928654.2, AL135999.1, PTOV1-AS2, AC090589.3, AC005253.1, AF117829.1, ARHGAP27P1-BPTFP1-KPNA2P3, AC009948.2, LINC00115, RUSC1-AS1,SNHG10, AL133243.3, AC245052.4, RAD51-AS1, LINC01409, AL162586.1,* and *AC006435.2*) were significantly highly expressed in tumor tissue.

Consensus clustering of m6A-related lncRNAs correlates with prognosis and biological functions in ccRCC

We adopted the resampling method to sample 80% of the samples and used the K-Means clustering algorithm to select the k value with the highest intracluster correlation, i.e., k = 2, as the optimal number of clusters, based on the results of k typing from 2 to 9 (Figure S1A-C). A total of 530 ccRCC patients were classified into 2 subtypes, namely, cluster 1 (n = 315) and cluster 2 (n = 215) (Figure 2A). The prognoses of clusters 1 and 2 were significantly different, and the survival rate for cluster 2 was lower than that for cluster 1 ($p < 0.001$, Figure 2B). Twenty-four high-risk m6A-related lncRNAs were highly expressed in cluster 2, and there were no significant differences in age, sex, grade, stage, or TNM staging between the 2 genotypes (Figure 2C).

To evaluate the potential biological functions of m6A-related lncRNAs, GO enrichment analysis and KEGG pathway enrichment analysis were conducted. The KEGG results showed that the mammalian Target of Rapamycin (mTOR) signaling pathway (NES = 1.81, NOM $p < 0.012$), ATP-binding cassette (ABC) transporter (NES = 1.76, NOM $p < 0.011$), Notch signaling pathway (NES = 1.74, NOM $p < 0.039$), and vascular endothelial growth factor (VEGF) signaling pathway (NES = 1.62, and NOM $p < 0.024$) were

significantly enriched in cluster 2 (Figure 2D). GO enrichment results showed that biological processes related to protein methylation (NES = 2.17, NOM p < 0.002), regulation of microtubule-based movement (NES = 2.05, NOM p < 0.001) and phospholipid acid metabolism (NES = 2.34, NOM p < 0.001) were significantly enriched in cluster2 (Figure 2E).

Consensus clustering of m6A-related lncRNAs correlates with immune genes

To explore the association between m6A-related lncRNAs and immunotherapy, we evaluated the differential expression of 6 types of immune checkpoints between the 2 subtypes and the correlation between immune checkpoints and m6A-related lncRNAs. We found that the expression levels of *PD-1, PD-L1, CTLA-4, LAG-3, TIM-3,* and *TIGIT* in tumor samples were significantly higher than those in normal samples (all p < 0.001) and the expression levels of *PD-1, PD-L1, and CTLA. -4, LAG-3,* and *TIGIT* in cluster 2 were significantly higher than those in cluster 1 (Figure 3A-F). *PD-1, PD-L1, CTLA-4, LAG-3,* and *TIGIT* were all positively correlated with m6A-related lncRNAs. *PD-1* expression was positively correlated with *AC084018.1, AC012615.6, AC114730.3, LINC00342, AL136295.7, AC004148.1, AL135999.1, PTOV1-AS2, AC090589.3, AC005253.1, ARHGAP27P1-BPTFP1-KPNA2P3, LINC00115, RUSC1-AS1, AC245052.4, RAD51-AS1, LINC01409, AL162586.1,* and *AC006435.2*. *TIM-3* was negatively correlated with *AL136295.7, AC004148.1, AL928654.2, ARHGAP27P1-BPTFP1-KPNA2P3, LINC00115, SNHG10, AC245052.4,* and *AC006435.2* (Figure 3G, H, Figure S2A-D).

Consensus clustering of m6A-related lncRNAs correlates with immune infiltration

In the TME, in addition to tumor cells, there are many nontumor components closely related to the biological processes of tumors, including stromal cells and immune cells. Using the unique properties of the transcription profile of tumor samples, we can predict the content of stromal cells and immune cells, i.e., the immune score and stromal score; the higher the score, the greater is the proportion of the corresponding components. Finally, the tumor purity of each tumor sample was calculated based on the sum of the 2 (ESTIMATE score); the higher the score, the lower is the tumor purity. The content of stromal cells in cluster 1 was higher than that in cluster 2 (p = 0.045). However, there were no significant differences in the percentage of immune cells and tumor purity between the 2 (Figure 4A-C).

In addition, we analyzed the infiltration of 22 immune cells in 2 subtypes and found that the infiltration of naive B cells and neutrophils in cluster 1 was high, while the infiltration of CD8 T cells, follicular helper T cells and resting NK cells in cluster 2 was more significant. In addition, although T regulatory cells (Tregs) were not significantly different between the 2 subtypes, the infiltration was more significant in cluster 2 (Figure 4D, E).

Construction and validation of the prognostic risk model

The ccRCC patients in the TCGA database were randomly divided into a training set (n = 266) and a test set (n = 264). There was no significant difference in the clinical baseline characteristics between the training set and the test set (p > 0.05, Table S3). LASSO regression analysis was performed for the

prognostic m6A-related lncRNAs (Figure S3A, B). Seven m6A-related lncRNAs were obtained: *LINC00342, AC018752.1, RPL34-AS1, AF117829.1, AC009948.2, SNHG10,* and *AL133243.3*. The 7 lncRNAs were used to construct a prognostic model to obtain a risk score formula for each sample: risk score = (*LINC00342* × 0.0554) - (*AC018752.1* × 0.1872) - (*RPL34-AS1* × 4.5020) + (*AF117829.1* × 0.3137) + (*AC009948.2* × 0.9556) + (SNHG10 × 0.0863) + (*AL133243.3* × 0.3944).

Based on the median risk score, patients in the training set were divided into high- and low-risk groups for Kaplan-Meier survival analysis. The results showed that the prognosis of patients in the high-risk group was lower than that of patients in the low-risk group ($p < 0.001$, Figure 5A). The AUCs at 1 year, 3 years, and 5 years were 0.729, 0.762, and 0.777, respectively, indicating that this model could well predict the prognosis of patients (Figure 5B). To further verify the accuracy of the prognostic model, we used it to analyze the test set. The results showed that the survival rates for patients in the high-risk and low-risk groups were significantly different ($p < 0.001$, Figure 5C); the AUCs were 0.69, 0.664, and 0.706, respectively, suggesting that the prognostic model had excellent sensitivity and specificity (Figure 5D).

The risk score curve, survival status, and heat map of gene expression for patients in the high-risk and low-risk groups are shown in Figure 5E-F. As the risk score increased, ccRCC patient deaths increased. In high-risk patients, 5 high-risk lncRNAs (*LINC00342, AF117829.1, AC009948.2, SNHG10,* and *AL133243.3*) were upregulated, and 2 low-risk lncRNAs (*AC018752.1* and *RPL34-AS1*) were downregulated; in contrast, the expression levels of these lncRNAs in low-risk patients were opposite.

Next, we performed univariate and multivariate Cox regression analyses to evaluate the prognostic value of risk scores and other clinical features of the prognostic model. Univariate Cox regression analysis indicated that age, grade, stage, and risk score were correlated with the prognosis of ccRCC patients (Figure 5G-H). Multivariate Cox regression analysis suggested that the risk score could be used as an independent prognostic risk factor (training set, $p < 0.001$; test set, $p = 0.002$; Figure 5I-J).

Prognostic risk score correlates with clinicopathological characteristics

We further performed Kaplan-Meier survival analysis of different ages, sex, grades, stages, and TNM stages and compared the survival rates for high- and low-risk patients in all stratifications to explore whether our prognostic model is suitable for patients within different clinical stratifications. The results are shown in Figure 6A-G. In older age (>65 years) or younger age (≤65 years) patients, males or females, with poorly differentiated or undifferentiated tumors (G3-4), different tumor sizes and infiltration depths (T1-2, T3-4), no lymph node (N0) or distant metastasis (M0), and early stage (stage I-II) or advanced stage (stage III-IV) disease, the survival rate of high risk patients significantly decreased. These results indicated that the m6A-related lncRNA-based prognostic model is a powerful tool for predicting the prognosis of ccRCC patients within different clinical stratifications.

Finally, we analyzed the correlation of risk scores with different clinicopathological characteristics and found that risk scores were significantly different among different clusters, grades, immune scores, TNM staging, and stage. Risk scores were significantly higher for patients in cluster 2, G3-4, low immune

scores, T3-4, N1, and M1 staging, and stage III-IV (Figure 7A-J), suggesting that the expression of m6A-related lncRNAs is related to the occurrence and development of ccRCC and that the model may be able to predict the progression of ccRCC.

Prognostic risk score correlates with immune checkpoint expression and immune cell infiltration

To determine whether our risk model could reflect the conditions of patients' immune microenvironment and to provide guidance for immunotherapeutic efficacy, we analyzed the differential expression of immune checkpoints among patients with different risks and the relationship between the risk score and immune cell infiltration. The expression levels of 6 immune checkpoints, i.e., *PD-1, PD-L1, CTLA-4, LAG-3, TIM-3*, and *TIGIT*, were significantly increased in the high-risk group (Figure 8A). The contents of memory B cells, CD8 T cells, follicular helper T cells, and Tregs were positively correlated with risk scores. The contents of these cells increased in ccRCC tissue with increased risk score. However, the other immune cell types, i.e., naive B cells, activated dendritic cells, resting dendritic cells, resting mast cells, monocytes, and resting memory CD4 T cells, were negatively correlated with risk score (Figure 8B).

Discussion

lncRNAs have been confirmed to be abnormally expressed in a variety of malignant tumors and to participate in tumor occurrence, development, invasion, and metastasis. lncRNAs play important mediating roles in cancer signal transduction pathways by interacting with proteins, RNAs and lipids [31]. Because lncRNAs have high organ and cell specificity, they can be found in many tissues and body fluids of patients. Some specific lncRNAs can be used as novel tumor biomarkers for tumor diagnosis, prognostic evaluation, therapeutic targets, and drug sensitivity prediction [32-33]. m6A modification is the most abundant epigenetic methylation modification in mammalian mRNAs and lncRNAs [34], affecting almost every process of RNA metabolism, including mRNA processing, translation and the biological occurrence of lncRNAs [35]. The m6A modification of lncRNAs plays an important regulatory role in the occurrence and development of a variety of cancers. For example, the level of m6A of the lncRNA NEAT1-1 can effectively predict the risk of death of prostate cancer patients, and high levels of m6A of NEAT1-1 is related to prostate cancer bone metastasis [36]. METTL3-mediated and METTL14-mediated m6A modification enhances the stability of LNCAROD in head and neck squamous cell carcinoma (HNSCC) cells, an effect that is associated with the high expression of LNCAROD in HNSCC [37]. Here, we identified 7 m6A-related lncRNAs that were significantly correlated with the prognosis of ccRCC patients and used those lncRNAs to construct a reliable risk model to predict the prognosis of patients and the TME, information that has certain guiding significance for tumor immunotherapy.

In this study, 27 prognostic m6A-related lncRNAs were identified by analyzing gene expression data of 530 ccRCC patients in the TCGA database. Among those 27 lncRNAs, 24 high-risk lncRNAs were highly expressed in tumor tissue, suggesting that these lncRNAs might have carcinogenic effects in the occurrence and development of ccRCC. The expression of these lncRNAs was significantly positively correlated with the m6A writers *RBM15* and *METTL3. RBM15* binds the m6A complex and recruits it to a

special RNA site [38]. *METTL3* is the first m6A methyltransferase that has been extensively studied in tumors and plays a major catalytic role in the m6A addition process [39]. *METTL3* can promote tumorigenesis and malignant progression, is highly expressed in a variety of malignant tumors, such as bladder cancer, breast cancer, and lung cancer, and is an indicator of poor patient prognosis [40-42]. It was found that the expression of METTL3-induced lncRNAs *ABHD11-AS1* and *LINC00958* was upregulated in non-small cell lung cancer (NSCLC) and liver cancer tissues and cells and closely associated with the poor prognosis of patients [43-44]. To investigate the biological characteristics of these m6A-related lncRNAs associated with prognosis, we classified, via consensus clustering, ccRCC patients into 2 subtypes based on the expression of lncRNAs. We found that patients in cluster 2 with high expression of high-risk lncRNAs had a poor prognosis, suggesting that m6A-related lncRNAs can be used as biomarkers to predict the prognostic risk of ccRCC. In addition, cluster typing was closely related to immune checkpoints, stromal scores, and immune cell infiltration. In cluster 2 patients, the stromal score was low, the contents of stromal cells were low, and immune-inhibitory cell infiltration was more obvious; *PD-1, PD-L1, CTLA-4, LAG-3,* and *TIGIT* were highly expressed and positively correlated with m6A-related lncRNAs. These results suggest that prognostic m6A-related lncRNAs might become a signature for the assessment of the TME and immunotherapeutic effects.

To understand the regulatory mechanism of m6A-related lncRNAs in ccRCC, we performed pathway and functional enrichment analysis for clusters 1 and 2. The results showed that signaling pathways associated with tumor occurrence and development, drug resistance, and angiogenesis, such as the mTOR signaling pathway, Notch signaling pathway, VEGF signaling pathway, and ABC transporters, were enriched to varying degrees in cluster 2 patients with a poor prognosis. mTOR is regulated by a variety of cell signals, mainly through the phosphatidylinositol 3-kinase (PI3K)/Akt/mTOR pathway, to achieve cell proliferation, autophagy and apoptosis, among other regulatory functions. In many cancer types, the mTOR signaling pathway is abnormally activated and is involved in tumor formation, the regulation of immune cell differentiation and tumor metabolism [45]. Notch is widely expressed in many species and is highly evolutionarily conserved. It affects cell differentiation, proliferation and apoptosis and is associated with the occurrence and development of cancers. lncRNAs can not only participate in the NOTCH signaling pathway as regulatory factors of target genes but also affect the transcription of downstream genes in the nucleus [46]. ABC transporters are a family of energy-dependent transport proteins located on the cell membrane. ABC transporters can mediate the unidirectional efflux of antitumor drugs and cause multidrug resistance in tumors [47]. GO analysis indicated that m6A-related lncRNAs were involved in biological processes such as protein methylation, microtubule-based movement regulation, and phosphatidic acid metabolism.

Based on the above results, we can confirm that m6A-related lncRNAs are closely related to the prognosis and biological process of ccRCC patients. Therefore, based on univariate and multivariate Cox regression analyses, we ultimately obtained 7 m6A-related lncRNAs that were significantly correlated with prognosis (*LINC00342, AC018752.1, RPL34-AS1, AF117829.1, AC009948.2, SNHG10,* and *AL133243.3*) and constructed a prognosis risk model. Studies have found that long intergenic non-protein coding RNA 00342 (*LINC00342*) can regulate the growth, invasion and metastasis of colorectal cancer and NSCLC

cells and is closely associated with the poor prognosis of patients [48-49]. The lncRNA ribosomal protein L34 antisense RNA 1 (*RPL34-AS1*) is localized on human chromosome 4q25 and has antitumor effects in esophageal carcinoma and papillary thyroid carcinoma. RPL34-AS1 overexpression can inhibit tumor cell proliferation and invasion and promote apoptosis [50-51]. Small nucleolar RNA host gene 10 (SNHG10) has been reported to be an oncogenic lncRNA of gastric cancer, liver cancer, osteosarcoma and other malignancies [52-54]. It is highly expressed in a variety of malignant tumors and is involved in the proliferation, invasion, and metastasis of tumor cells. However, some studies also reported that the high expression of SNHG10 predicts a good prognosis for NSCLC patients [55].

Survival analysis, ROC curves and risk curves were used to analyze the accuracy and stability of the model; the results indicated that the model can accurately distinguish high- and low-risk patients and accurately predict the prognostic risk of ccRCC. The stratification of different clinical traits showed that this model could effectively predict the prognosis of patients of different ages, sex, and stages. Univariate and multivariate Cox regression analyses showed that this risk model could be used as an independent prognostic indicator for ccRCC patients. In addition, we also analyzed the relationship between the expression of prognostic m6A-related lncRNAs in the model and different clinicopathological characteristics. We found that the risk score was associated with the progression of ccRCC. In summary, our prognostic model is reliable and can be used to identify the risk and prognosis of ccRCC patients, information that is conducive to early intervention and treatment.

In recent years, immunotherapy targeting immune checkpoints has made substantial breakthroughs, bringing new hope to ccRCC patients. However, the complex microenvironment of tumors can mediate immune escape, leading to the failure of immunotherapy [56]. lncRNAs are overexpressed during the development, differentiation and activation of immune cells, such as macrophages, dendritic cells, neutrophils, T cells, B cells and bone marrow mesenchymal stem cells [57]. Recent studies have found that lncRNAs are involved in various processes of the immune response in the TME and the promotion of tumor immunosuppression [58] and play a role in the evaluation and measurement of the immunotherapeutic response in various cancers, such as endometrial cancer and liver cancer [59-60]. Huang et al. [61] found that the lncRNA NKILA alters the balance between immune activating and immunosuppressive T cell subsets in the TME by regulating the apoptosis sensitivity of T cell subsets, resulting in tumor immune escape. Wang et al. [62] showed that lncRNA-MALAT1 promotes the immune escape of diffuse large B-cell lymphoma by targeting miR-195. MALAT1 gene knockout promotes the proliferation of CD8+ T cells and inhibits the epithelial-mesenchymal transition (EMT)-like signal transduction process through Ras-extracellular signal-regulated kinase (RAS/ERK) signaling pathways. The lncRNA SNHG15 promotes PD-L1 expression through the inhibition of miR-141 and participates in the immune escape of gastric cancer [63]. Currently, there are limited studies that have investigated the effects of m6A-regulated lncRNAs on the immune microenvironment of ccRCC. In this study, we found that the expression levels of *PD-1, PD-L1, CTLA-4, LAG-3, TIM-3*, and *TIGIT* were higher in high-risk patients, who are more likely to benefit from immunotherapy. The risk score was positively correlated with the infiltration level of memory B cells, CD8 T cells, follicular helper T cells, and Tregs. The risk score was negatively correlated with the infiltration level of naive B cells, activated dendritic cells, resting dendritic

cells, resting mast cells, monocytes, and resting memory CD4 T cells. These results suggest that m6A-related lncRNAs are involved in the regulation of the immune microenvironment to a certain extent. Pan et al. [64] found that dendritic cells resting, dendritic cells activated, mast cells resting, mast cells activated and eosinophils are associated with favorable prognosis in patients with ccRCC, whereas B cells memory, T cells follicular helper and Tregs are correlated with poorer outcome.

This study has some limitations. First, the risk model constructed in this study was based on a public clinical database: TCGA. The results were confirmed in a TCGA cohort but lacked external validation. Therefore, further testing in larger multicenter clinical patient cohorts is needed in the future. In addition, the specific regulatory mechanism of the screened m6A-related lncRNAs in ccRCC requires further study.

Conclusion

This study systematically analyzed the prognostic value of m6A-related lncRNAs in ccRCC patients, as well as their significance in the assessment of the immune microenvironment and immunotherapeutic efficacy. A prognostic risk model based on 7 m6A-related lncRNAs was constructed and validated. The model can predict the prognosis of patients within different clinical stratifications and the progression of ccRCC. The risk score can be used as an independent prognostic indicator for ccRCC. In addition, the risk signals of m6A-related lncRNAs were related to the expression of immune checkpoints and immune cell infiltration. Our study provides a novel method for the individualized risk stratification of ccRCC patients, providing a basis for further exploring the mechanisms underlying the occurrence and development of ccRCC and potentially providing a target for improving the response to immunotherapy in patients with ccRCC.

List Of Abbreviations

RCC, renal cell carcinoma; ccRCC, clear cell renal cell carcinoma; lncRNA, long non-coding RNA; m6A, N6-methyladenosine; RNA-seq, transcriptomic sequencing; TCGA, The Cancer Genome Atlas; KEGG, Kyoto Encyclopedia of Genes and Genomes; GO, Gene Ontology; TME, tumor microenvironment; mTOR, mammalian Target of Rapamycin; VEGF, vascular endothelial growth factor; NES, normalized enrichment score; PD-1, programmed cell death 1; PD-L1, programmed cell death-Ligand 1; CTLA-4, cytotoxic T lymphocyte-associated antigen 4; LAG-3, lymphocyte activation gene-3; TIM3, T cell immunoglobulin and mucin domain-containing protein 3; TIGIT, T cell immunoglobulin and ITIM domain.

Declarations

Ethics approval and consent to participate

The data of the patients in this study were obtained from the public database datasets, and written informed consent was obtained from these patients.

Consent for publication

All authors approved the manuscript and consent publication.

Availability of data and materials

The authors declare that the data supporting the findings of this study are available in the TCGA database (https://portal.gdc.cancer.gov).

Competing interests

The authors declare that the research was conducted in the absence of any commercial or financial relationships that could be construed as a potential conflict of interest.

Funding

This work was supported by Beijing University of Chinese Medicine 2020 Basic Research Business Expenses Project (No.2020-JYB-ZDGG-143-1) and National Natural Science Foundation of China General Program (No.82074545).

Authors' contributions

JH and XJ conceived and designed the study; ZF and SZ downloaded and organized the TCGA data; YQ and XW performed data analysis and wrote the paper; JH and XJ critically revised the article for essential intellectual content and administrative support. All authors read and approved the final manuscript.

Acknowledgements

The authors would like to thank the TCGA databases for the availability of the data.

References

1. Siegel RL., Miller KD., Fuchs HE., Jemal A. Cancer Statistics, 2021. CA Cancer J Clin. 2021; 71:7-33.
2. Shuch B., Amin A., Armstrong AJ., Eble JN., Ficarra Vi, Lopez-Beltran A., et al. Understanding pathologic variants of renal cell carcinoma: distilling therapeutic opportunities from biologic complexity. Eur Urol. 2015;67:85-97.
3. di Martino S., De Luca G., Grassi L., Federici G., Alfonsi R., Signore M., et al. Renal cancer: new models and approach for personalizing therapy. J Exp Clin Cancer Res. 2018;37:217.
4. Attalla K., Weng S., Voss MH., Hakimi AA. Epidemiology, Risk Assessment, and Biomarkers for Patients with Advanced Renal Cell Carcinoma. Urol Clin North Am. 2020;47:293-303.
5. Ascierto PA., Addeo R., Cartenì G., Daniele B., De Laurentis M., Ianniello GP., et al. The role of immunotherapy in solid tumors: report from the Campania Society of Oncology Immunotherapy (SCITO) meeting, Naples 2014. J Transl Med. 2014;12:291.
6. Motzer RJ, Powles T, Atkins MB, Escudier B, McDermott DF, Suarez C, et al. IMmotion151: a randomized phase III Study of atezolizumab plus bevacizumab vs sunitinib in untreated meta-static

renal cell carcinoma (mRCC). J Clin Oncol. 2018;36:578

7. Flippot R., Escudier B., Albiges L. Immune Checkpoint Inhibitors: Toward New Paradigms in Renal Cell Carcinoma. Drugs. 2018;78:1443-1457.
8. Batista PJ., Chang HY. Long noncoding RNAs: cellular address codes in development and disease. Cell. 2013;152:1298-307.
9. Sahu A., Singhal U., Chinnaiyan AM. Long noncoding RNAs in cancer: from function to translation. Trends Cancer. 2015;1:93-109.
10. Haemmerle M., Gutschner T. Long non-coding RNAs in cancer and development: where do we go from here? Int J Mol Sci. 2015;16:1395-405.
11. Li YJ., Egranov SD., Yang LQ., Lin CR. Molecular mechanisms of long noncoding RNAs-mediated cancer metastasis. Genes Chromosomes Cancer. 2019;58:200-207.
12. Choudhari R., Sedano MJ., Harrison AL., Subramani R., Lin KY., Ramos EI., et al. Long noncoding RNAs in cancer: From discovery to therapeutic targets. Adv Clin Chem. 2020; 95:105-147.
13. Zhao JL., Wang CL., Liu YL., Zhang GY. Long noncoding RNA SNHG14 enhances migration and invasion of ovarian cancer by upregulating DGCR8. Eur Rev Med Pharmacol Sci. 2019; 23:10226-10233.
14. Zhuo W., Liu YM., Li S., Guo DY., Sun Q., Jin J., et al. Long Noncoding RNA GMAN, Up-regulated in Gastric Cancer Tissues, Is Associated With Metastasis in Patients and Promotes Translation of Ephrin A1 by Competitively Binding GMAN-AS. Gastroenterology. 2019; 156: 676-691.
15. Wang W., Hu WT., Wang Y., An Y., Song L., Shang PT., et al. Long non-coding RNA UCA1 promotes malignant phenotypes of renal cancer cells by modulating the miR-182-5p/DLL4 axis as a ceRNA. Mol Cancer. 2020;19:18.
16. He LE., Li HY., Wu AQ., Peng YL., Shu G., Yin G. Functions of N6-methyladenosine and its role in cancer. Mol Cancer. 2019;18:176.
17. Wang TY., Kong S., Tao M., Ju SQ. The potential role of RNA N6-methyladenosine in Cancer progression. Mol Cancer. 2020;19:88.
18. Wang Y., Cong R., Liu SY., Zhu B., Wang X., Xing Q. Decreased expression of METTL14 predicts poor prognosis and construction of a prognostic signature for clear cell renal cell carcinoma. Cancer Cell Int. 2021;21:46.
19. Wang YY., Zhang YJ., Du YS., Zhou MQ., Zhang SZ. Emerging roles of N6-methyladenosine (mA) modification in breast cancer. Cell Biosci. 2020;10:136.
20. Meyer KD, Saletore Y, Zumbo P, Elemento O, Mason CE, Jaffrey SR. Comprehensive analysis of mRNA methylation reveals enrichment in 3' UTRs and near stop codons. Cell. 2012;149:1635-1646.
21. Chen Y., Lin Y., Shu YQ., He J., Gao W. Interaction between N-methyladenosine (mA) modification and noncoding RNAs in cancer. Mol Cancer. 2020;19:94.
22. Tu ZW., Wu L., Wang P., Hu Q., Tao CM., Li KX., et al. N6-Methylandenosine-Related lncRNAs Are Potential Biomarkers for Predicting the Overall Survival of Lower-Grade Glioma Patients. Front Cell

Dev Biol. 2020;8:642.

23. Jiang XL., Liu BY., Nie Z., Duan LC., Xiong QX., Jin ZX., et al. The role of m6A modification in the biological functions and diseases. Signal Transduct Target Ther. 2021;6:74.
24. Li YS., Xiao J., Bai J., Tian Y., Qu YW., Chen X., et al. Molecular characterization and clinical relevance of mA regulators across 33 cancer types. Mol Cancer. 2019;18:137.
25. Wilkerson, M.D., Hayes, D.N. ConsensusClusterPlus: a class discovery tool with confidence assessments and item tracking. Bioinformatics. 2010;26:1572-3.
26. Ritchie ME, Phipson B, Wu D, Hu Y, Law CW, Wei S, et al. limma powers differential expression analyses for RNA-sequencing and microarray studies. Nucleic Acids Res. 2015;43:e47-e47.
27. Wei TY, Viliam S. R package "corrplot": Visualization of a Correlation Matrix (Version 0.84). 2017; Available from https://github.com/taiyun/corrplot.
28. Newman AM., Liu CL., Green MR., Gentles AJ., Feng WG., Xu Y., et al. Robust enumeration of cell subsets from tissue expression profiles. Nat Methods. 2015;12:453-7.
29. Kosuke Y., Hoon K., Roel GW V. estimate: Estimate of Stromal and Immune Cells in Malignant Tumor Tissues from Expression Data. R package version 1.0.13/r21. 2016; Available from https://R-Forge.R-project.org/projects/estimate/
30. Max Kuhn. caret: Classification and Regression Training. R package version 6.0-86. 2020; Available from https://CRAN.R-project.org/package=caret
31. Lin CR., Yang LQ. Long Noncoding RNA in Cancer: Wiring Signaling Circuitry. Trends Cell Biol. 2018;28:287-301.
32. Sarfi M., Abbastabar M., Khalili E. Long noncoding RNAs biomarker-based cancer assessment. J Cell Physiol. 2019;234:16971-16986.
33. Wei L., Wang XW., Lv LY., Zheng Y., Zhang NA., Yang M. The emerging role of noncoding RNAs in colorectal cancer chemoresistance. Cell Oncol (Dordr). 2019;42:757-768.
34. Liu N., Parisien M., Dai Q., Zheng GQ., He C., Pan T. Probing N6-methyladenosine RNA modification status at single nucleotide resolution in mRNA and long noncoding RNA. RNA. 2013;19:1848-56.
35. Dai DJ., Wang HY., Zhu LY., Jin HC, Wang X. N6-methyladenosine links RNA metabolism to cancer progression. Cell Death Dis. 2018;9:124.
36. Wen SM., Wei YL., Zen C., Xiong W., Niu YJ., Zhao Y. Long non-coding RNA NEAT1 promotes bone metastasis of prostate cancer through N6-methyladenosine. Mol Cancer. 2020;19:171.
37. Ban YY., Tan PQ., Cai J., Li JJ., Hu M., Zhou Y., et al. LNCAROD is stabilized by m6A methylation and promotes cancer progression via forming a ternary complex with HSPA1A and YBX1 in head and neck squamous cell carcinoma. Mol Oncol. 2020;14:1282-1296.
38. Patil DP., Chen CK., Pickering BF., Chow A., Jackson C., Guttman M., et al. m(6)A RNA methylation promotes XIST-mediated transcriptional repression. Nature. 2016;537:369-373. doi:10.1038/nature19342

39. Jiang XL., Liu BY., Nie Z., Duan LC., Xiong QX., Jin ZX., et al. The role of m6A modification in the biological functions and diseases. Signal Transduct Target Ther. 2021;6:74.
40. Han J, Wang JZ, Yang X, Yu H, Zhou R, Lu HC, et al. METTL3 promote tumor proliferation of bladder cancer by accelerating pri-miR221/222 maturation in m6A-dependent manner. Mol Cancer. 2019;18:110.
41. Wang H, Xu B, Shi J. N6-methyladenosine METTL3 promotes the breast cancer progression via targeting Bcl-2. Gene. 2020;722:144076.
42. Wanna-Udom S, Terashima M, Lyu H, Ishimura A, Takino T, Sakari M, et al. The m6A methyltransferase METTL3 contributes to Transforming Growth Factor-beta-induced epithelial-mesenchymal transition of lung cancer cells through the regulation of JUNB. Biochem Biophys Res Commun. 2020;524:150-155.
43. Xue L., Li J., Lin YH., Liu DG., Yang Qi., Jian JT., et al. m A transferase METTL3-induced lncRNA ABHD11-AS1 promotes the Warburg effect of non-small-cell lung cancer. J Cell Physiol. 2021;236:2649-2658.
44. Zuo XL., Chen ZQ., Gao W., Zhang Y., Wang JG., Wang JF., et al. M6A-mediated upregulation of LINC00958 increases lipogenesis and acts as a nanotherapeutic target in hepatocellular carcinoma. J Hematol Oncol. 2020;13:5.
45. Zou Z, Tao T, Li H, Zhu X. mTOR signaling pathway and mTOR inhibitors in cancer: progress and challenges. Cell Biosci. 2020;10:31.
46. Guo J., Li P., Liu XM., Li YL. NOTCH signaling pathway and non-coding RNAs in cancer. Pathol Res Pract. 2019;215:152620.
47. Szakács G., Paterson JK., Ludwig JA., Booth-Genthe C., Gottesman MM. Targeting multidrug resistance in cancer. Nat Rev Drug Discov. 2006;5:219-34.
48. Shen P., Qu LL., Wang JJ., Ding QC., Zhou CW., Xie R., et al. LncRNA LINC00342 contributes to the growth and metastasis of colorectal cancer via targeting miR-19a-3p/NPEPL1 axis. Cancer Cell Int. 2021;21:105.
49. Chen QF., Kong JL., Zou SC., Gao H., Wang F., Qin SM., et al. LncRNA LINC00342 regulated cell growth and metastasis in non-small cell lung cancer via targeting miR-203a-3p. Eur Rev Med Pharmacol Sci. 2019;23:7408-7418.
50. Ji LL., Fan X., Zhou F., Gu J., Deng XD. ncRNA RPL34-AS1 inhibits cell proliferation and invasion while promoting apoptosis by competitively binding miR-3663-3p/RGS4 in papillary thyroid cancer. J Cell Physiol. 2020;235:3669-3678.
51. Gong Z., Li J., Cang P., Jiang HC., Liang JW., Hou YL. RPL34-AS1 functions as tumor suppressive lncRNA in esophageal cancer. Biomed Pharmacother. 2019;120:109440.
52. Yuan X., Yang TW., Xu Y., Ou S., Shi., Cao M., et al. SNHG10 Promotes Cell Proliferation and Migration in Gastric Cancer by Targeting miR-495-3p/CTNNB1 Axis. Dig Dis Sci. 2020; doi:10.1007/s10620-020-06576-w.

53. Lan T, Yuan K. LncRNA SNHG10 facilitates hepatocarcinogen-esis and metastasis by modulating its homolog SCARNA13 via a positive feedback loop. Cancer Res. 2019;79:3220-3234
54. Zhu ST., Liu Y., Wang X., Wang JY., Xi GH. lncRNA SNHG10 Promotes the Proliferation and Invasion of Osteosarcoma via Wnt/β-Catenin Signaling. Mol Ther Nucleic Acids. 2020;22: 957-970.
55. Liang M., Wang LL., Cao CH., Song SM., Wu F. LncRNA SNHG10 is downregulated in non-small cell lung cancer and predicts poor survival. BMC Pulm Med. 2020;20:273.
56. Osipov A., Saung MT., Zheng L., Murphy AG. Small molecule immunomodulation: the tumor microenvironment and overcoming immune escape. J Immunother Cancer. 2019;7:224.
57. Safarzadeh E, Asadzadeh Z, Safaei S, Hatefi A, Derakhshani A, Giovannelli F, et al. MicroRNAs and lncRNAs-A New Layer of Myeloid-Derived Suppressor Cells Regulation. Front Immunol. 2020;11:572323.
58. Luo Y., Yang JQ., Yu J., Liu XW., Yu C., Hu JP., et al. Long Non-coding RNAs: Emerging Roles in the Immunosuppressive Tumor Microenvironment. Front Oncol. 2020;10:48.
59. Liu JH., Mei J., Wang YC., Chen XC., Pan JD., Tong LG., et al. Development of a novel immune-related lncRNA signature as a prognostic classifier for endometrial carcinoma. Int J Biol Sci. 2021;17:448-459.
60. Zhang YQ., Zhang LM., Xu YW., Wu XY., Zhou Y., Mo JG. Immune-related long noncoding RNA signature for predicting survival and immune checkpoint blockade in hepatocellular carcinoma. J Cell Physiol. 2020;235:9304-9316.
61. Huang D., Chen JN., Yang LB., Ouyang Q., Li JQ., Lao LY.,et al. NKILA lncRNA promotes tumor immune evasion by sensitizing T cells to activation-induced cell death. Nat Immunol. 2018;19:1112-1125.
62. Wang QM., Lian GY., Song Y., Huang YF., Gong Y. LncRNA MALAT1 promotes tumorigenesis and immune escape of diffuse large B cell lymphoma by sponging miR-195. Life Sci. 2019;231:116335.
63. Dang SC., Malik A., Chen JX., Qu JG., Yin K., Cui L., et al. LncRNA SNHG15 Contributes to Immuno-Escape of Gastric Cancer Through Targeting miR141/PD-L1. Onco Targets Ther. 2020;13:8547-8556.
64. Pan QF, Wang LW, Chai SS, Zhang H, Li B. The immune infiltration in clear cell Renal Cell Carcinoma and their clinical implications: A study based on TCGA and GEO databases. J Cancer. 2020;11: 3207-3215.

Figures

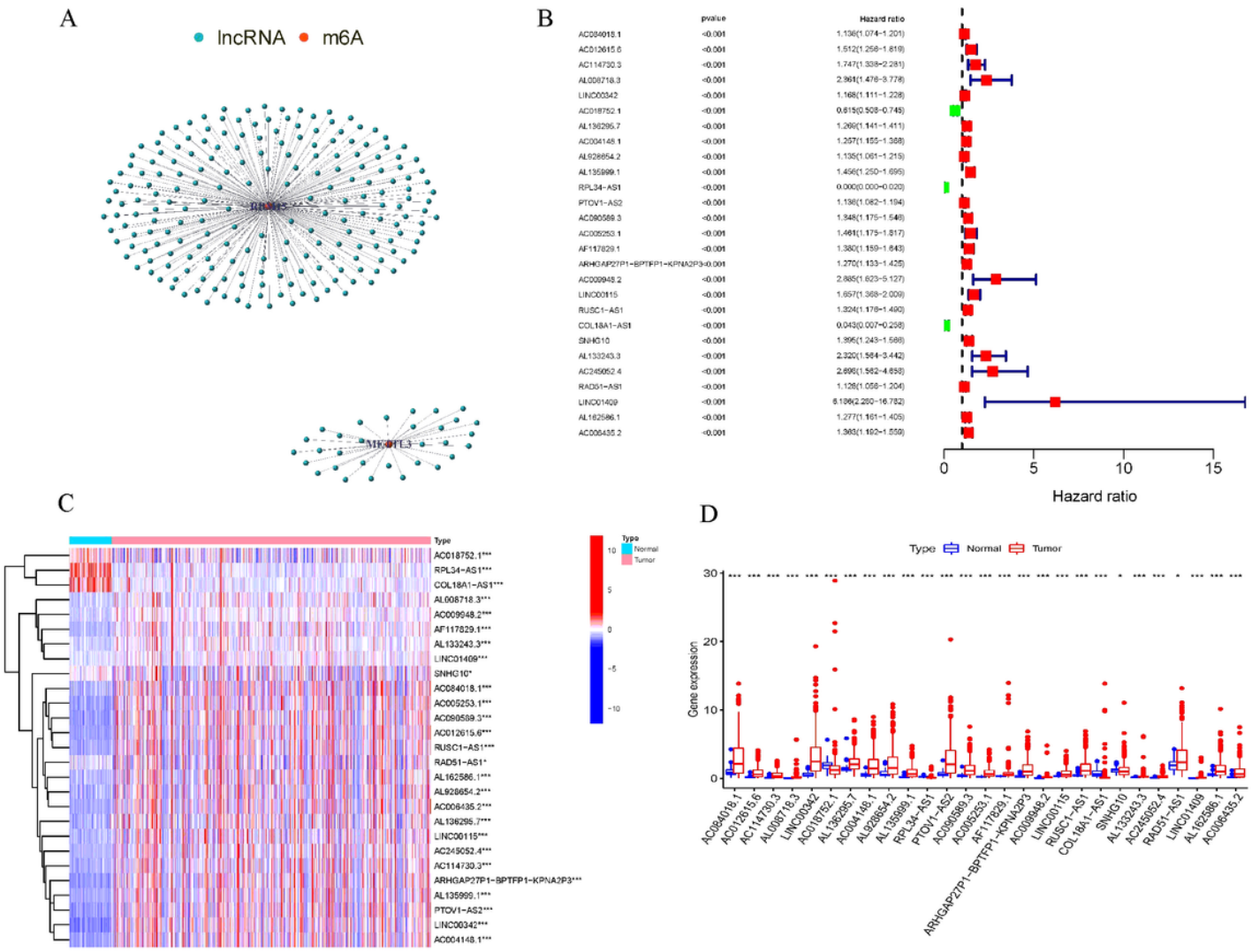

Figure 1

Identification of m6A-related lncRNAs associated with ccRCC prognosis. (A) Co-expression map of m6A and lncRNAs. (B) The forest plot of screening prognostic-related m6A-related lncRNAs by univariate Cox regression analysis. The heat map (C) and box plot (D) of the expression of 27 m6A-related lncRNAs in tumors and normal tissues. *p <0.05, **p < 0.01, and ***p < 0.001.

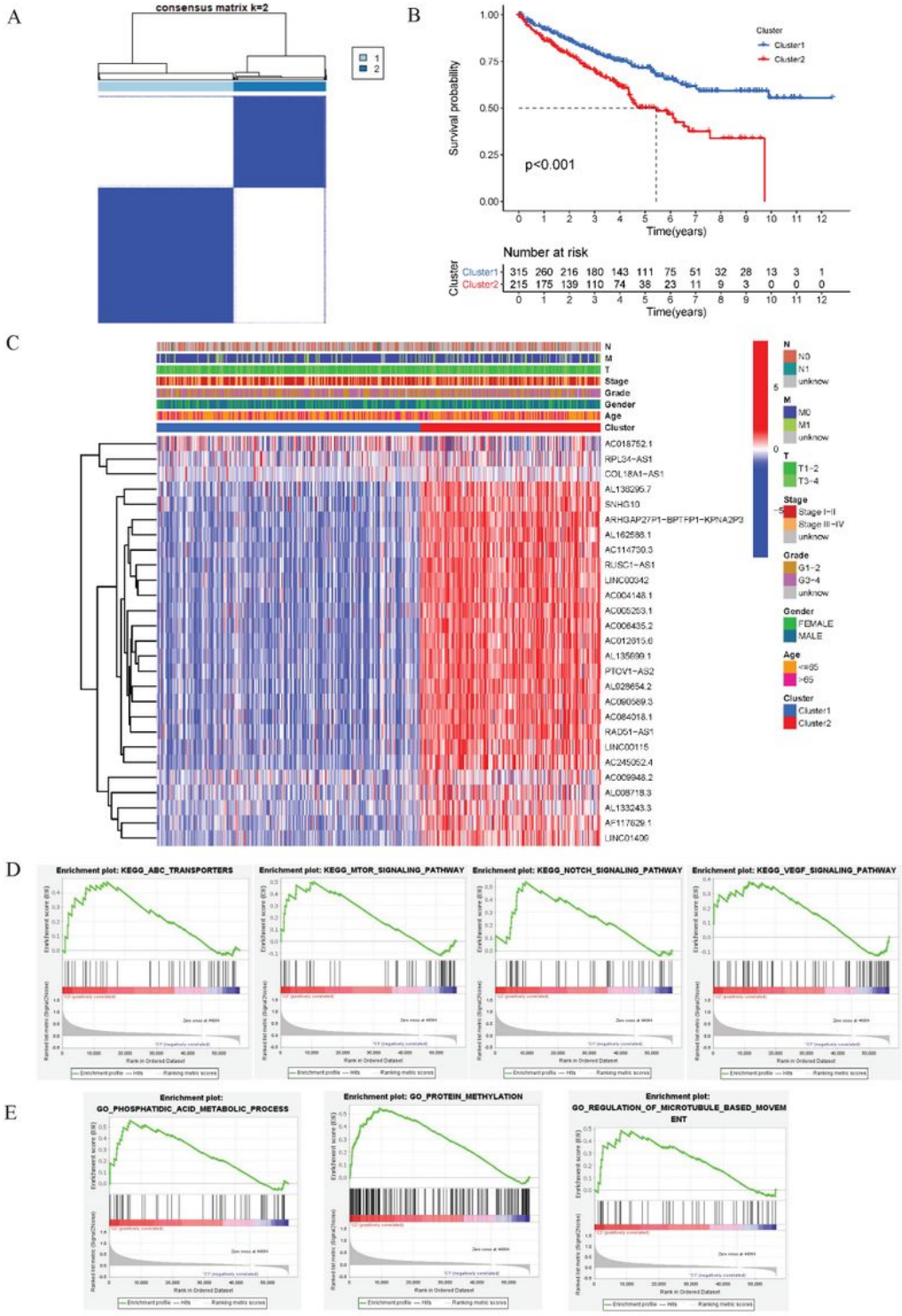

Figure 2

Consensus clustering of m6A-related lncRNAs correlates with clinicopathological features and biological functions in ccRCC. (A) Consensus clustering matrix for k = 2. (B) Kaplan-Meier survival analysis of ccRCC patients in two clusters. (C) The heatmap of clinicopathologic features of the two clusters. (D) KEGG results showed that the mTOR signaling pathway, ABC transporter, Notch signaling pathway and VEGF signaling pathway are significantly enriched in cluster 2. (E) GO results showed that biological

processes related to protein methylation, regulation of microtubule-based movement and phospholipid acid metabolism are significantly enriched in cluster2.

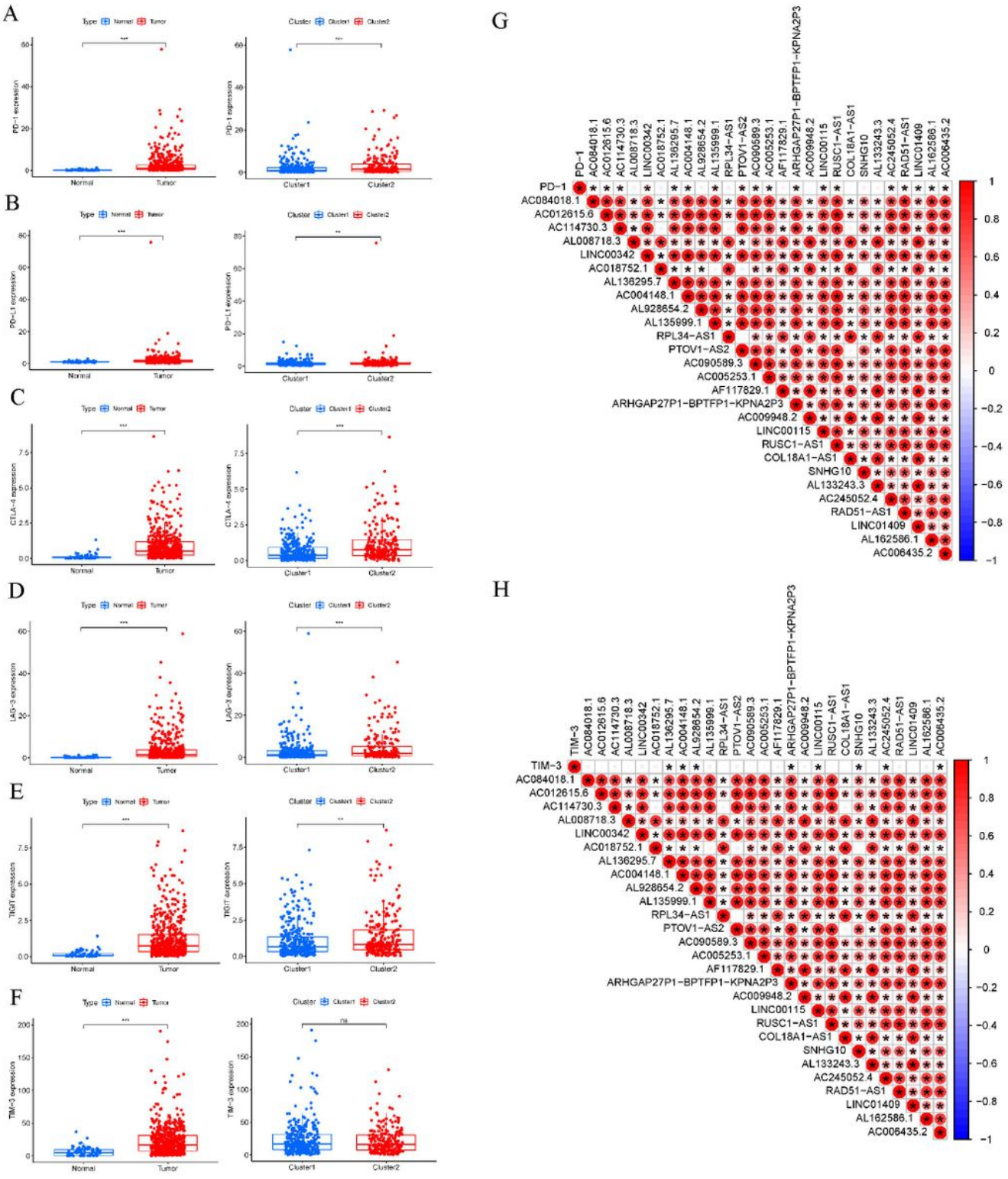

Figure 3

Association of immune checkpoints with m6A-related lncRNAs in ccRCC. (A) PD-1, (B) PD-L1, (C) CTLA-4, (D) LAG-3, (E) TIGIT and (F) TIM-3 expression difference between normal and ccRCC tumor tissues and

cluster1 and 2. The correlation of (G) PD-1 and (H) TIM-3 with m6A-related lncRNAs. *p <0.05, **p < 0.01, and ***p < 0.001.

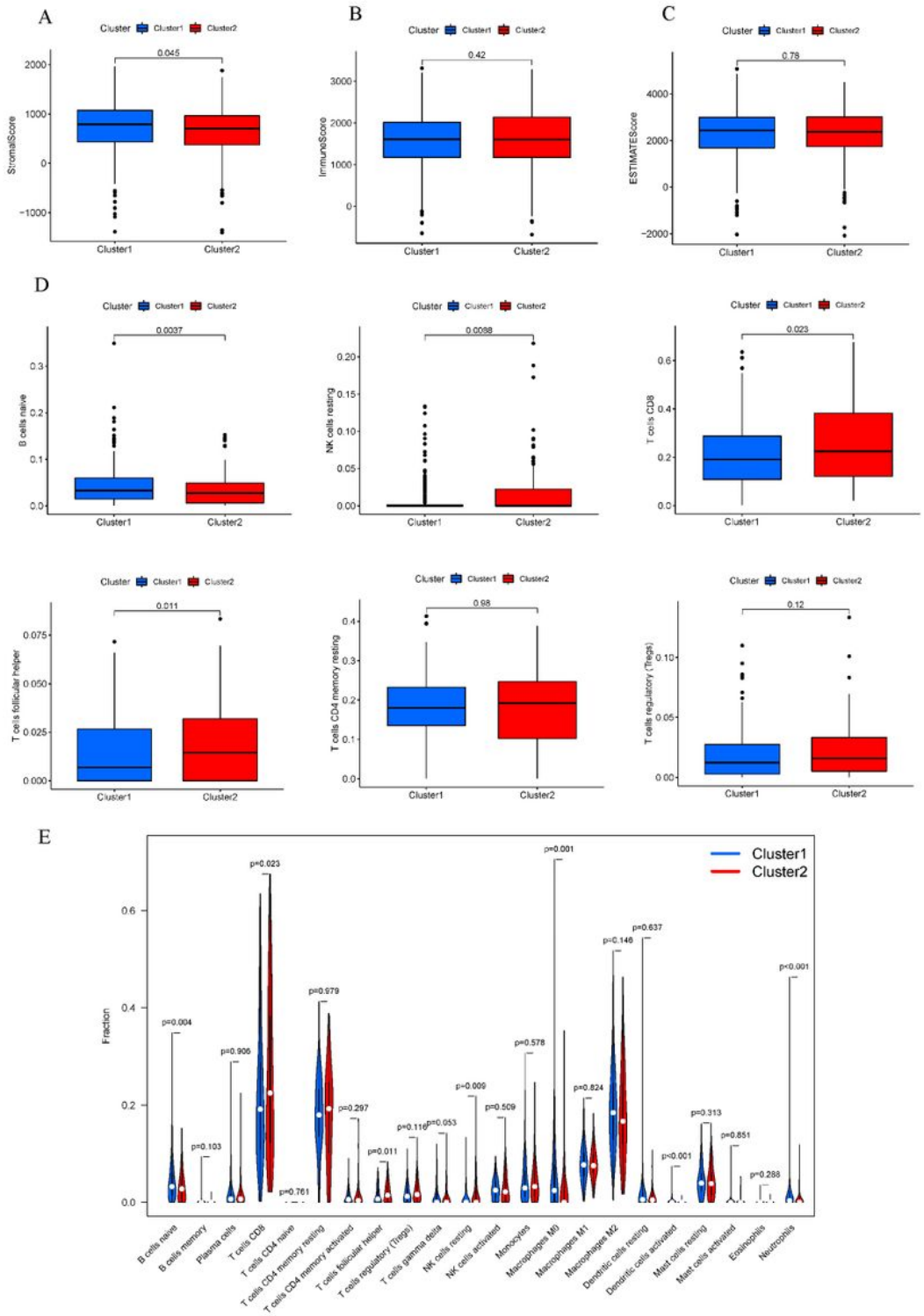

Figure 4

Association of tumor microenvironment and immune cell infiltration with m6A-related lncRNAs in ccRCC. (A) Stromal score, (B) immune score and (C) ESTIMATE score of cluster1/2. (D) Differences in immune cell infiltration between cluster 1/2. (E) The infiltrating levels of 22 immune cell types in cluster1/2.

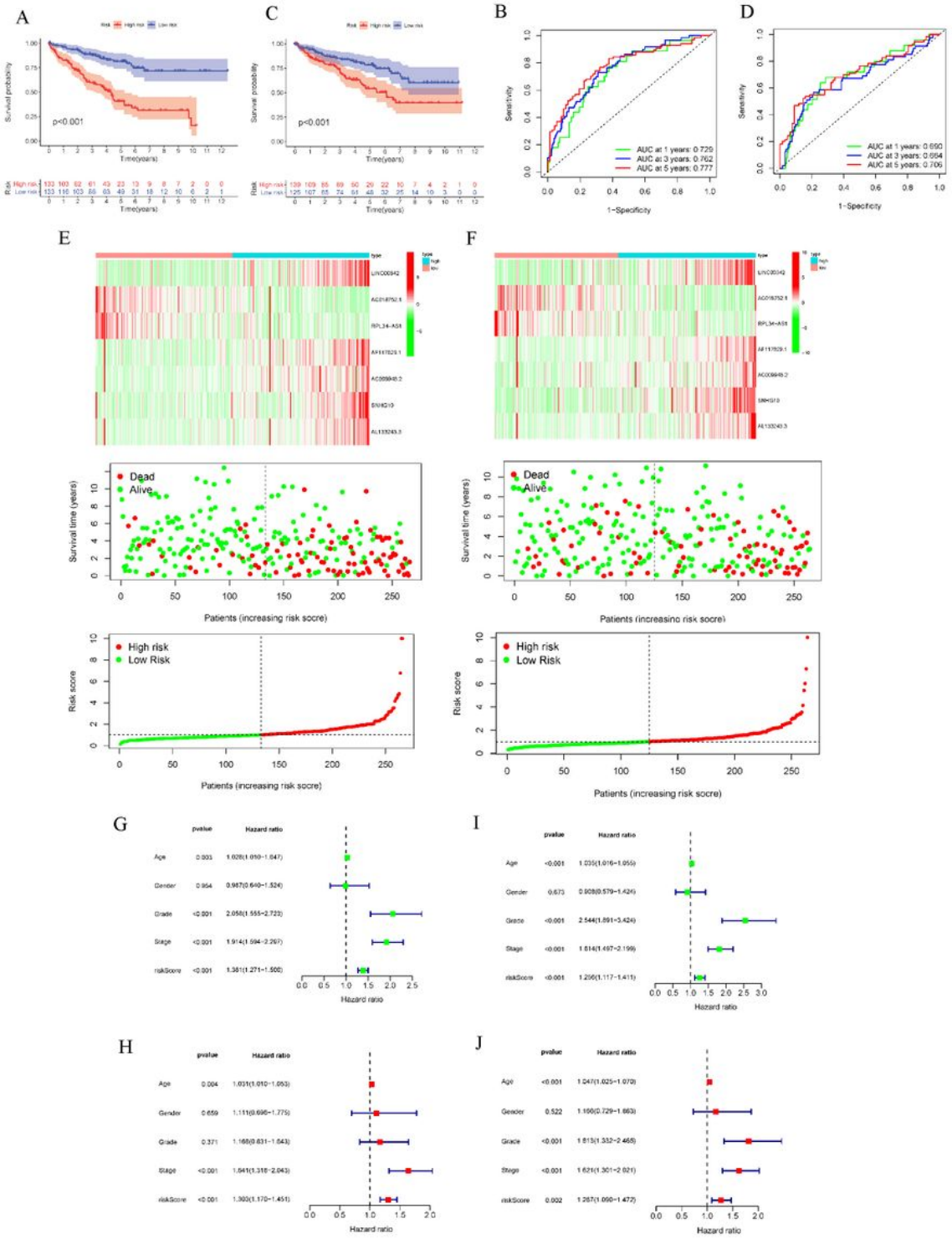

Figure 5

Construction and validation of the prognostic risk model. (A, C) Kaplan-Meier curves and (B, D) ROC analysis of the prognostic model in train set and test set. (E, F) Heat map, survival status and risk score curve of ccRCC patients in train set and test set. The (G, I) univariate and (H, J) multivariate Cox regression analysis of evaluating the independent prognostic value of the risk score of the prediction model.

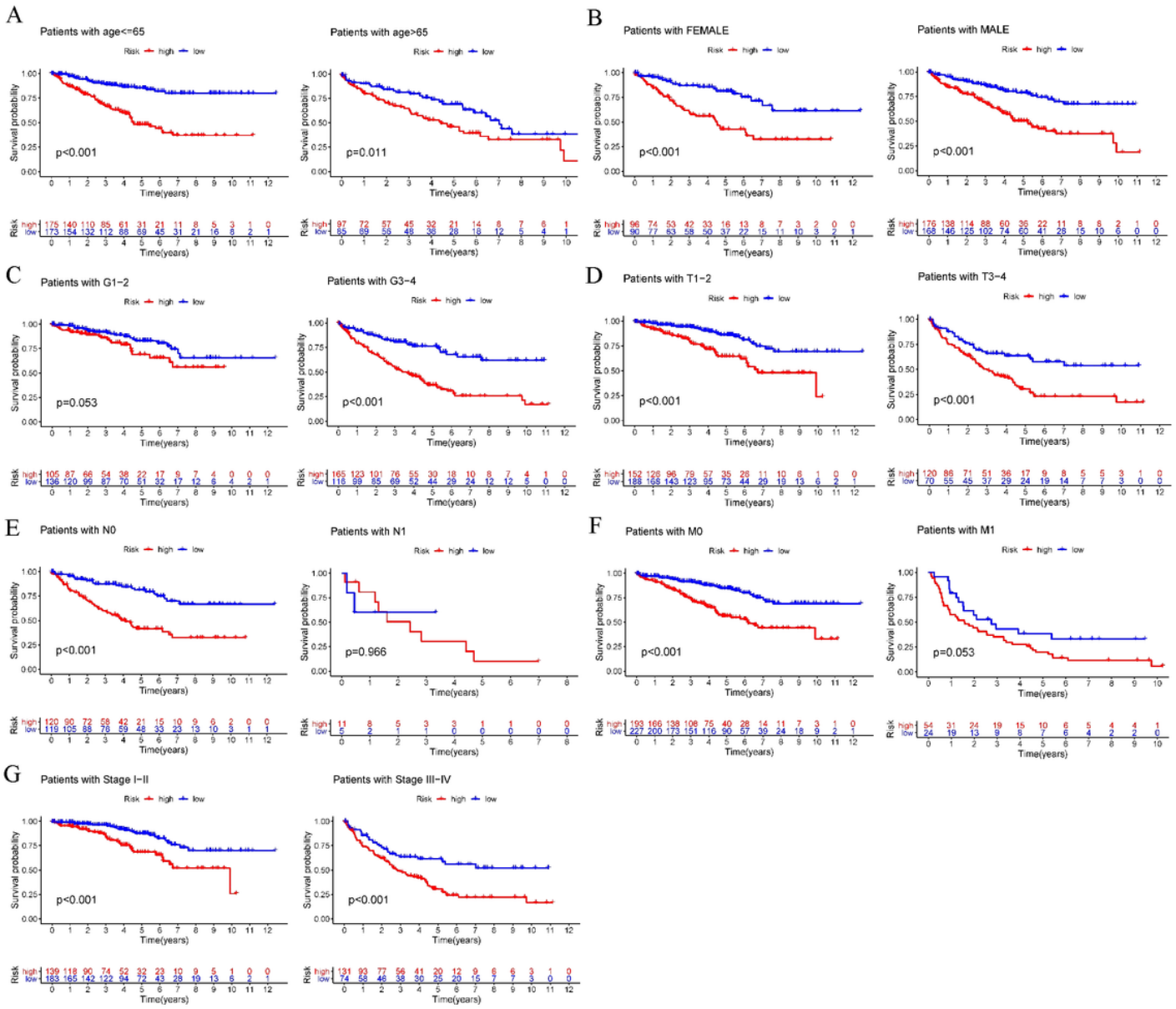

Figure 6

Kaplan-Meier survival analysis of the prognostic risk score for ccRCC stratified by clinicopathological characteristics. (A) age ≤65 / >65 years; (B) female and male; (C) patients with G1-2/G3-4; (D) patients with T1-2/T3-4; (E) patients with N0/N1; (F) patients with M0/M1; (G) patients with Stage I-II/III-IV.

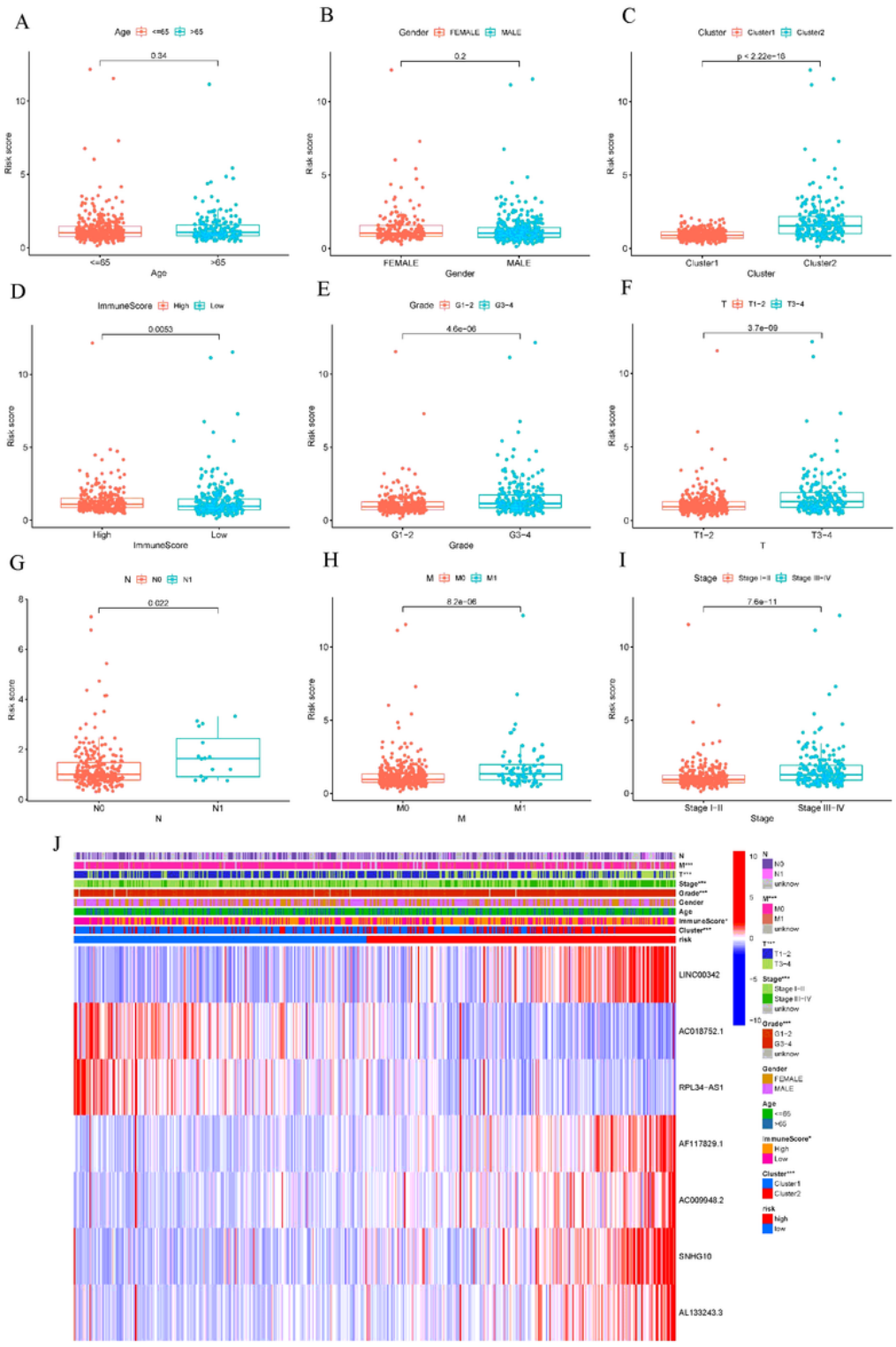

Figure 7

The correlation of risk score with the clinicopathological characters of ccRCC. (A) age ≤65 vs. >65 years; p = 0.34; (B) male vs. female; p = 0.2; (C) cluster1 vs. cluster2; p < 2.22e-16; (D) high immune score vs. low immune score; p = 0.0053; (E) G1-2 vs. G3-4; p = 4.6e-06; (F) T1-2 vs. T3-4; p = 3.7e-09; (G) N0 vs. N1; p = 0.022; (H) M0 vs. M1; p = 8.2e-06; (I) Stage I-II vs. III-IV; p = 7.6e-11.

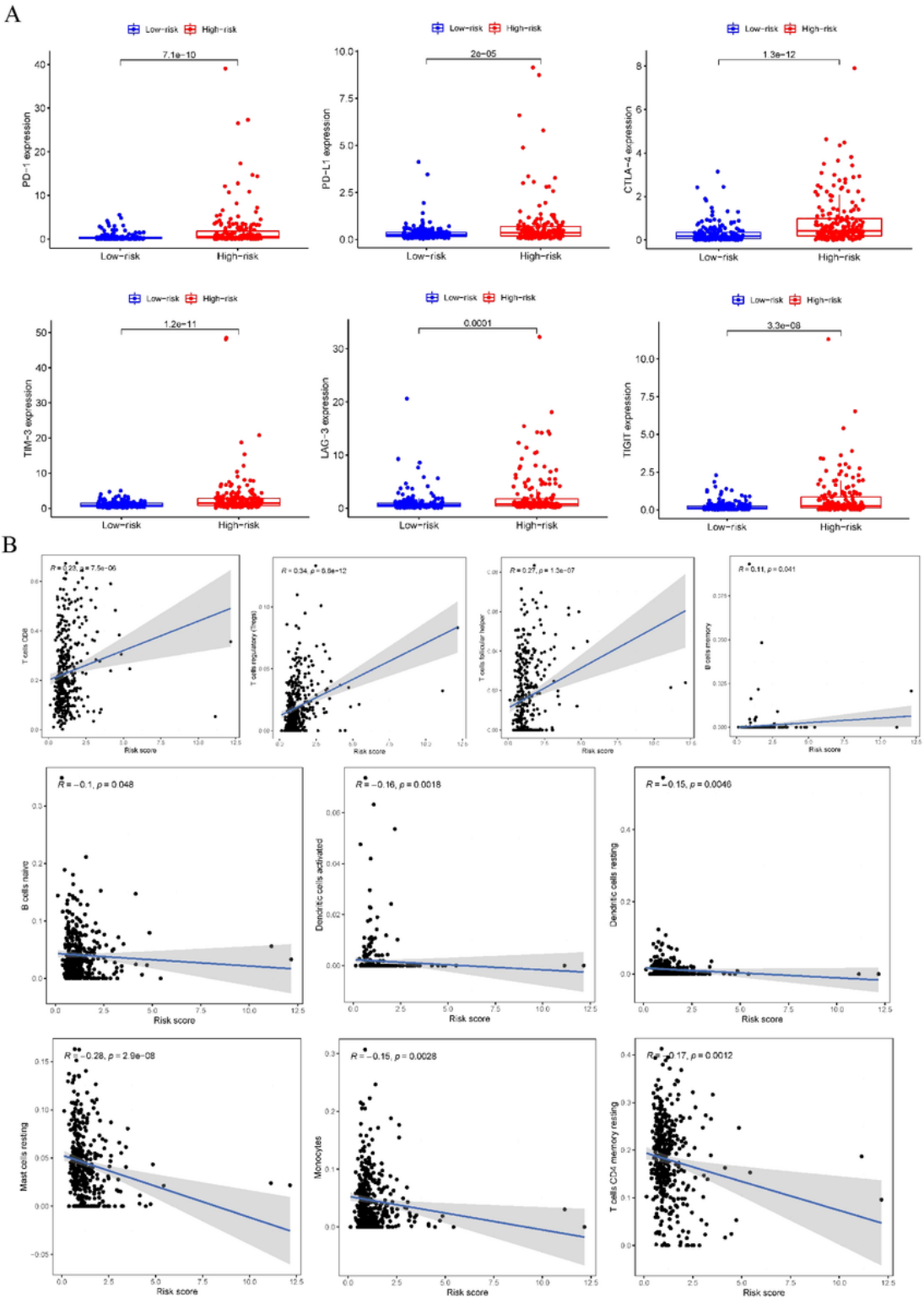

Figure 8

Association of prognostic risk scores with immune checkpoints and immune cell infiltration. (A) PD-1, PD-L1, CTLA-4, LAG-3, TIM-3, and TIGIT are significantly increased in the high-risk group. (B) The contents of memory B cells, CD8 T cells, follicular helper T cells, and Tregs were positively correlated with risk scores, whereas naive B cells, activated dendritic cells, resting dendritic cells, resting mast cells, monocytes, and resting memory CD4 T cells, were negatively correlated with risk score.

Supplementary Files

This is a list of supplementary files associated with this preprint. Click to download.

- FigureS1S3.pdf
- TableS1S3.docx